Electronic Supplementary Material (ESI) for Lab on a Chip.

Supplemental Information

Proof-of-concept optimization of a copper-mediated ^{18}F-radiosynthesis of a novel MAGL PET tracer on a high-throughput microdroplet platform and its macroscale translation

Yingqing Lu[abc], Yingfang He[d], Roger Schibli[d], Linjing Mu[d], R. Michael van Dam*[abc]

[a]Crump Institute for Molecular Imaging, University of California Los Angeles (UCLA), Los Angeles, CA, USA

[b]Department of Molecular & Medical Pharmacology, UCLA, Los Angeles, CA, USA

[c]Physics and Biology in Medicine Interdepartmental Graduate Program, UCLA, Los Angeles, CA, USA

[d]Center for Radiopharmaceutical Sciences, Institute of Pharmaceutical Sciences, Department of Chemistry and Applied Biosciences, ETH Zurich, Zurich, Switzerland

Contents

1 Optimization of [^{18}F]YH149 synthesis on droplet reactors

1.1 Initial conditions

Table S1. Results of initial experiments. **Condition 1** was adapted from the macroscale conditions reported by He et al. for the Cu-mediated radiosynthesis of [^{18}F]YH149[1] by reducing reagent amounts by 10x (30x for $Cu(OTf)_2(Py)_4$) and volume by 30x. **Condition 2** was taken from a previous study where we optimized the Cu-mediated radiofluorination step for [^{18}F]FDOPA, and we simply changed the precursor to that for [^{18}F]YH149[2]. Abbreviations: PTC = phase transfer catalyst.

Adapted reference condition	**1**	**2**
PTC (amount (µmol))	K_{222} (1.7), $K_2C_2O_4$ (0.6)	TEAOTf (0.3)
Base (amount (µmol))	K_2CO_3 (0.07)	Cs_2CO_3 (0.01)
Amount of precursor (µmol) [mg]	0.45 [0.24]	0.45 [0.24]
Amount of $Cu(OTf)_2(Py)_4$ (µmol)	0.68	0.68
10 µL of solvent	DMA/nBuOH (2:1, v/v)	DMA/Py (96:4, v/v)
Temperature (°C)	110	110
Reaction time (min)	5	5
Radiosynthesis performance (n = 2)		
Starting activity (MBq)	45 ± 1	46 ± 1
Fluorination conversion (%)	0	44 ± 1
Collection efficiency (%), decay-corrected	84 ± 1	81 ± 2
Crude RCY (%), decay-corrected	0	36 ± 2

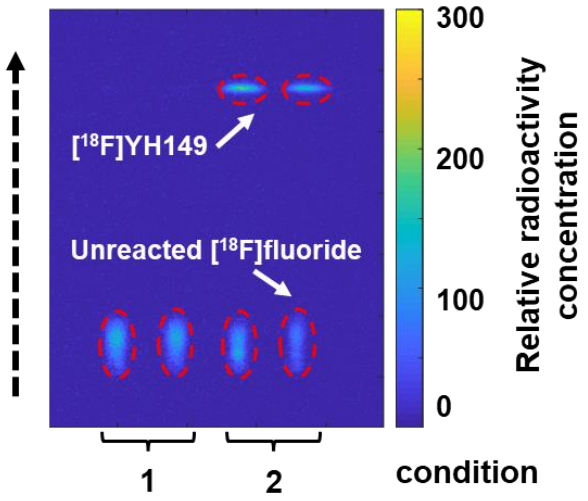

Figure S1. Analysis of crude fluorination products from initial experiments using multi-lane TLC with Cerenkov luminescence imaging (CLI) readout.

1.2 Influence of solvent type

Table S2. Impact of fluorination solvent on the performance of the droplet radiosynthesis of [^{18}F]YH149.

Solvent[a]	Fluorination conversion (%)	Collection efficiency (%)	Crude RCY (%)
DMF	11 ± 2	64 ± 4	7 ± 1
DMA	43 ± 3	69 ± 3	29 ± 3
DMSO	3 ± 0	70 ± 2	2 ± 0
NMP	36 ± 1	75 ± 6	27 ± 2
DMA/nBuOH (v/v, 2:1)	49 ± 2	75 ± 1	35 ± 0
DMA/nBuOH (v/v, 2:1)[b]	0	84 ± 1	0

[a]All reactions were performed with 0.3 µmol of TEAOTf, 0.01 µmol of Cs_2CO_3, 0.18 µmol of precursor and 0.68 µmol of $Cu(OTf)_2(Py)_4$ in 10 µL of solvent/pyridine (96:4, v/v) at 110°C for 5 min (n = 3 replicates each condition). [b]The reaction was performed in the absence of pyridine (n = 2 replicates).

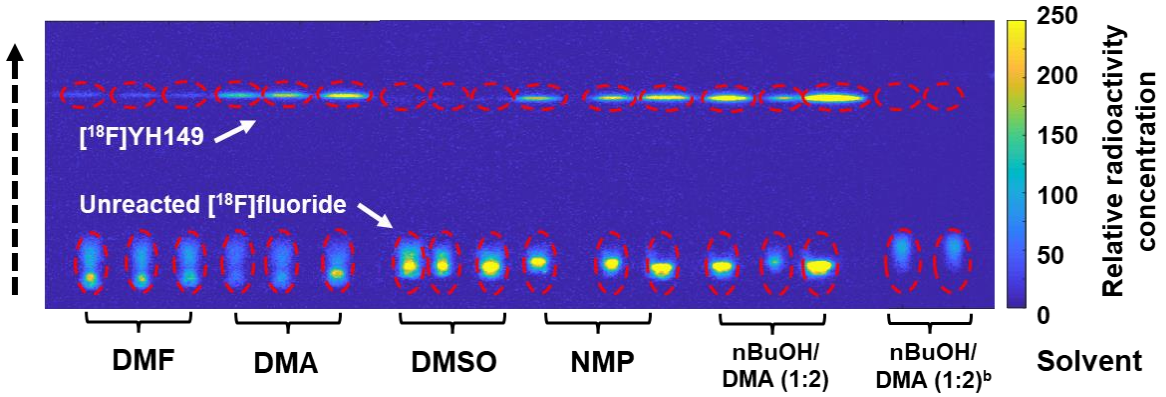

Figure S2. High-throughput analysis of crude fluorination products (from study of solvent) using multi-lane TLC with CLI readout.

1.3 Influence of type of phase transfer catalyst (PTC)/base

Table S3. Impact of type of PTC/base on the performance of the droplet radiosynthesis of [^{18}F]YH149.

PTC/base[a]	Fluorination conversion (%)	Collection efficiency (%)	Crude RCY (%)
TEAOTf/Cs_2CO_3	44 ± 3	71 ± 3	31 ± 3
TBAOTf/Cs_2CO_3	36 ± 2	73 ± 8	26 ± 4
TEAOTf	36 ± 1	70 ± 1	25 ± 1
TBAOTf	28 ± 7	66 ± 6	19 ± 6
$TBAHCO_3$	18 ± 1	77 ± 2	14 ± 1

[a]All reaction was performed with 0.3 µmol of PTC, 0.01 µmol of Cs_2CO_3 (if applied), 0.18 µmol of precursor and 0.68 µmol of $Cu(OTf)_2(Py)_4$ in 10 µL of DMA/nBuOH/pyridine (64:32:4, v/v) at 110°C for 5 min (n = 3 replicates each condition).

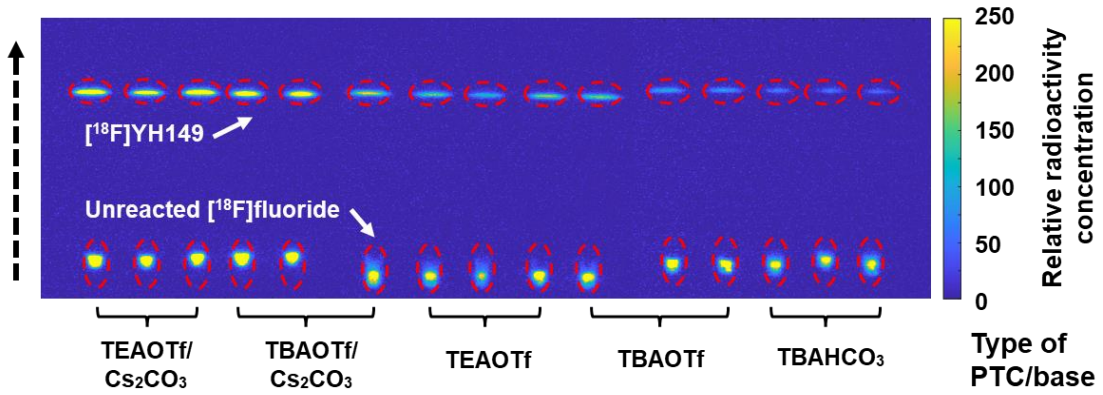

Figure S3. High-throughput analysis of crude fluorination products (from study of PTC/base type) using multi-lane TLC with CLI readout.

1.4 Impact of fluorination temperature and base type

Table S4. Impact of fluorination temperature (when using TEAOTf/Cs_2CO_3) on the performance of the droplet radiosynthesis of [^{18}F]YH149.

Fluorination temperature (°C)[a]	Fluorination conversion (%)	Collection efficiency (%)	Crude RCY (%)
100	29 ± 1	70 ± 0	21 ± 1
110	49 ± 1	68 ± 1	33 ± 1
115	58 ± 1	65 ± 2	38 ± 2
120	64 ± 4	63 ± 2	40 ± 2
130	70 ± 4	59 ± 4	41 ± 5
140	78 ± 1	55 ± 1	43 ± 1

[a]All reaction was performed with 0.3 µmol of PTC, 0.01 µmol of Cs_2CO_3, 0.18 µmol of precursor and 0.68 µmol of $Cu(OTf)_2(Py)_4$ in 10 µL of DMA/nBuOH/pyridine (64:32:4, v/v) at investigating temperature for 5 min (n = 3 replicates each condition).

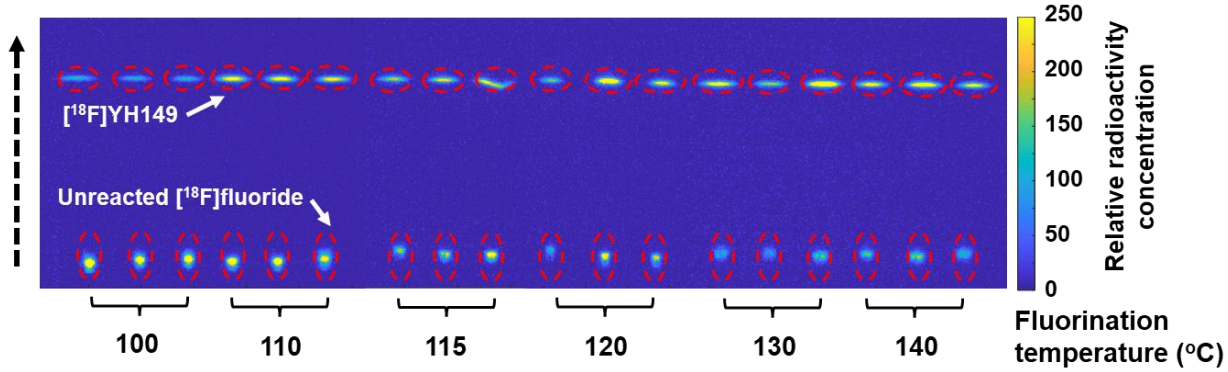

Figure S4. High-throughput analysis of crude fluorination products (from study of reaction temperature with TEAOTf/Cs_2CO_3) using multi-lane TLC with CLI readout.

Table S5. Impact of fluorination temperature (when using TEAOTf/K_2CO_3) on the performance of the droplet radiosynthesis of [^{18}F]YH149.

Fluorination temperature (°C)[a]	Fluorination conversion (%)	Collection efficiency (%)	Crude RCY (%)
120	66 ± 3	59 ± 2	39 ± 3
140	67 ± 1	57 ± 3	38 ± 2
150	68 ± 1	52 ± 2	35 ± 1
160	58 ± 4	46 ± 4	26 ± 2

[a]All reaction was performed with 0.3 µmol of PTC, 0.01 µmol of K_2CO_3, 0.18 µmol of precursor and 0.68 µmol of $Cu(OTf)_2(Py)_4$ in 10 µL of DMA/nBuOH/pyridine (64:32:4, v/v) at investigating temperature for 5 min (n = 3 replicates each condition).

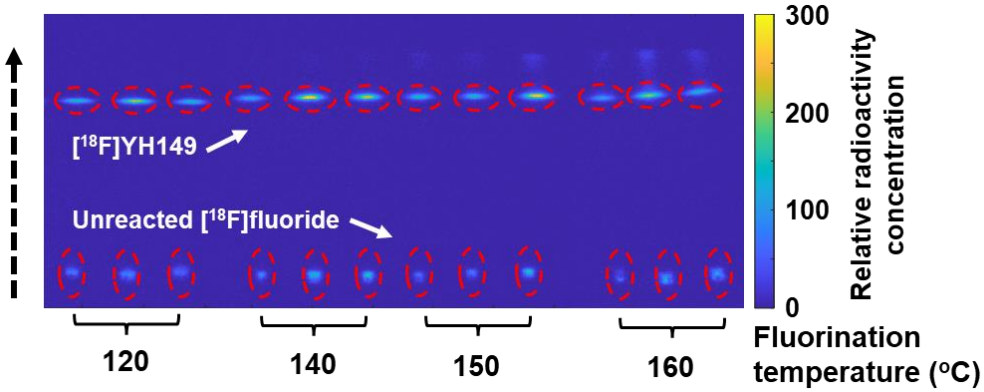

Figure S5. High-throughput analysis of crude fluorination products (from study of reaction temperature with TEAOTf/K_2CO_3) using multi-lane TLC with CLI readout.

1.5 Impact of reaction time

Table S6. Impact of reaction time on the performance of the droplet radiosynthesis of [^{18}F]YH149.

Reaction time (min)[a]	Fluorination conversion (%)	Collection efficiency (%)	Crude RCY (%)
0.5	35 ± 1	74 ± 0	26 ± 1
1	41 ± 2	63 ± 0	26 ± 2
2	61 ± 1	63 ± 3	39 ± 2
3	66 ± 3	64 ± 0	42 ± 2
5	68 ± 1	52 ± 2	36 ± 2
7	73 ± 6	49 ± 3	36 ± 5

[a]All reaction was performed with 0.3 µmol of PTC, 0.01 µmol of K_2CO_3, 0.18 µmol of precursor and 0.68 µmol of $Cu(OTf)_2(Py)_4$ in 10 µL of DMA/nBuOH/pyridine (64:32:4, v/v) at 140°C for investigating reaction time (n = 3 replicates each condition).

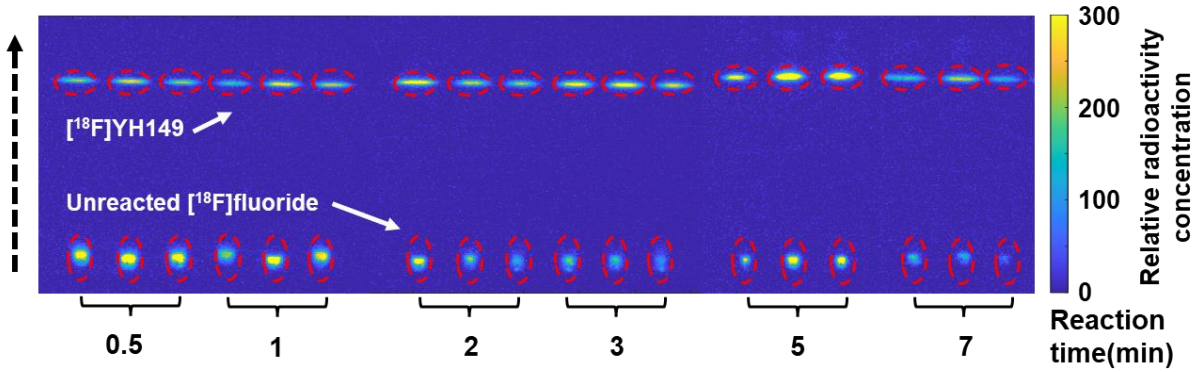

Figure S6. High-throughput analysis of crude fluorination products (from study of reaction time) using multi-lane TLC with CLI readout.

1.6 Influence of amount of base

Table S7. Impact of amount of base on the performance of the droplet radiosynthesis of [^{18}F]YH149.

Base amount (nmol)[a]	Fluorination conversion (%)	Collection efficiency (%)	Crude RCY (%)
10	73 ± 6	49 ± 3	36 ± 5
20[b]	68 ± 7	47 ± 1	32 ± 4
30[b]	61 ± 2	50 ± 2	30 ± 2

[a]All reaction was performed with 0.3 µmol of PTC, investigating amount of K_2CO_3, 0.18 µmol of precursor and 0.68 µmol of $Cu(OTf)_2(Py)_4$ in 10 µL of DMA/nBuOH/pyridine (64:32:4, v/v) at 140°C for 7 min (n = 3 replicates each condition). [b]n = 2 replicates each condition.

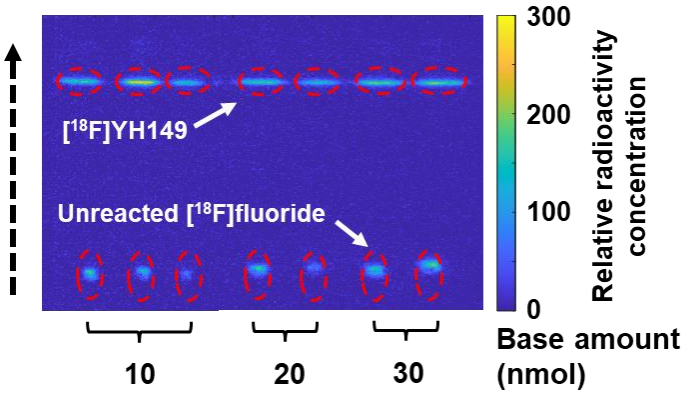

Figure S7. High-throughput analysis of crude fluorination products (from study of base amount with K_2CO_3) using multi-lane TLC with CLI readout.

1.7 Influence of amount of precursor

Table S8. Influence of amount of precursor on the performance of the droplet radiosynthesis of [^{18}F]YH149.

Amount of precursor (mg)[a]	Fluorination conversion (%)	Collection efficiency (%)	Crude RCY (%)
0.05	66 ± 0	53 ± 4	35 ± 2
0.1	64 ± 5	60 ± 6	38 ± 1
0.15	62 ± 2	68 ± 4	42 ± 4
0.15[b]	80 ± 2	71 ± 3	56 ± 3
0.15[c]	71 ± 5	57 ± 1	40 ± 4
0.2	60 ± 1	61 ± 2	36 ± 1
0.25	59 ± 2	61 ± 1	36 ± 1
0.3	64 ± 3	62 ± 2	39 ± 3

[a]All reaction was performed with 0.3 µmol of PTC, 0.01 µmol of K_2CO_3, investigating amount of precursor and 0.68 µmol of $Cu(OTf)_2(Py)_4$ in 10 µL of DMA/nBuOH (v/v, 2:1) along with 4% of pyridine (v/v) at 140°C for 3 min (n=3 replicates each condition). [b]The reaction was performed with Cs_2CO_3 instead of K_2CO_3, and was repeated n = 4 times. [c]The reaction was performed in presence of DMA/nBuOH/pyridine (64:32:4, v/v), and was repeated n = 4 times.

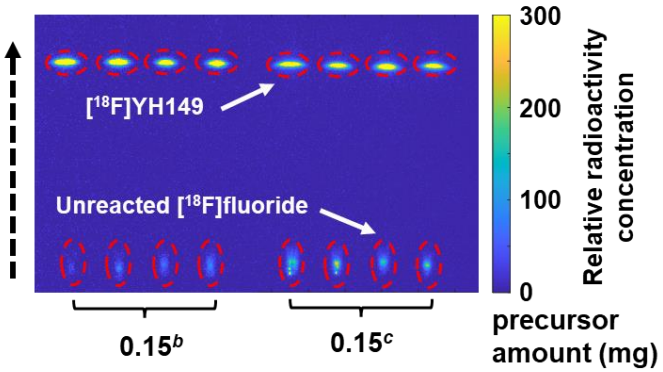

Figure S8. High-throughput analysis of crude fluorination products (from additional tested conditions) using multi-lane TLC with CLI readout. The conditions marked at the bottom are precursor amounts with superscripts matching the special cases from **Table S8**.

2 Macroscale synthesis performance

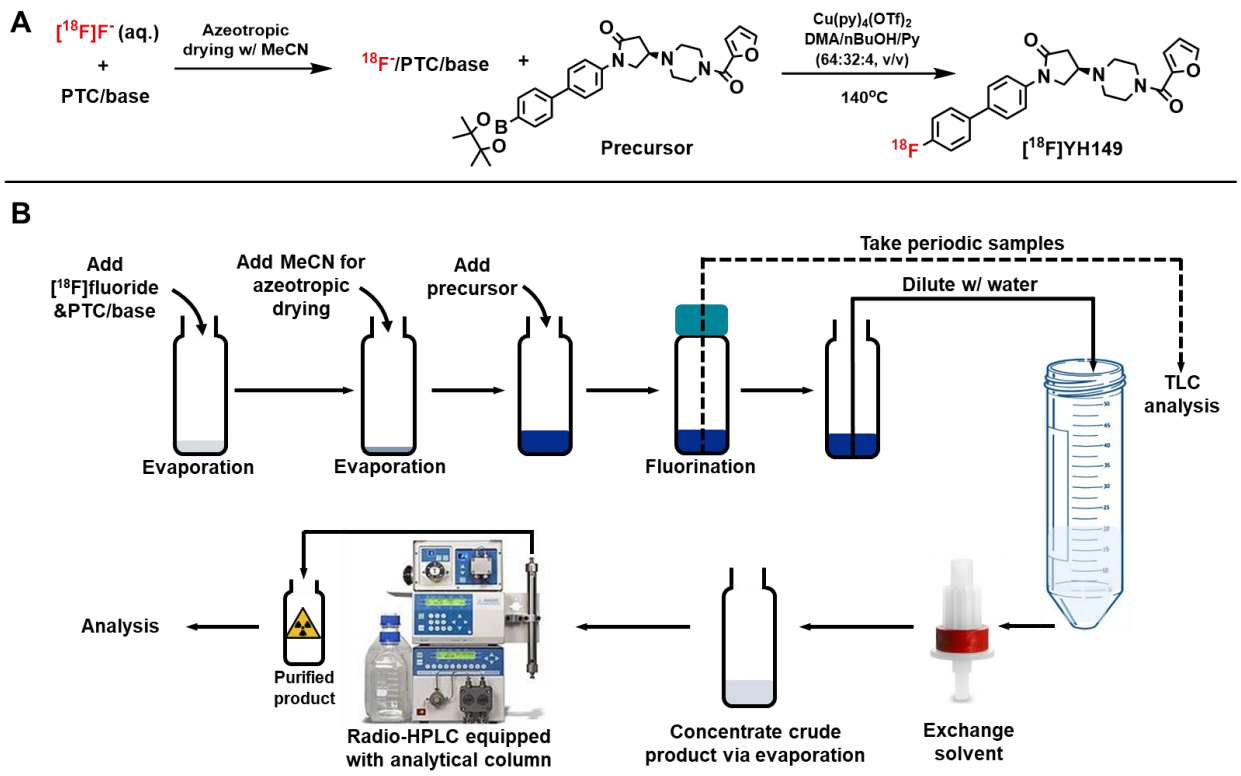

Figure S9. Implementation of radiosynthesis in a vial-based (macroscale) reaction.

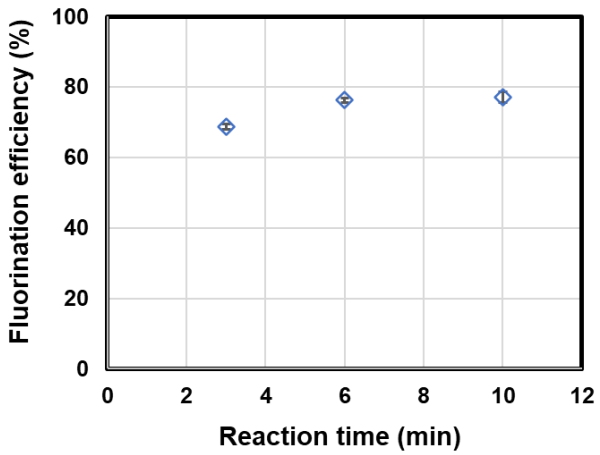

Figure S10. Impact on fluorination efficiency of different reaction times (n = 4) in the macroscale synthesis.

Table S9. Performance of translated (droplet to vial) radiosynthesis of [^{18}F]YH149. Activity measurements are expressed as fractions of starting activity (corrected for decay).

Process	Measurement	Result
[^{18}F]F$^-$ drying	Starting activity (GBq)	0.2-1.4
	Duration for evaporating initial 25 µL [^{18}F]F$^-$/PTC/base (min)	5
	Duration for cooling down (min)	1
	3 X Duration for additional MeCN (30 µL) azeotropic evaporation (min)	6
	3 X Duration for cooling down (min)	3
	Duration of the whole drying process (min)	15
Radio-fluorination	Activity of 3-min sample (%)	0.3 ± 0.2
	Activity of 6-min sample (%)	0.4 ± 0.2
	Activity of 10-min sample (%)	0.3 ± 0.2
	Collected activity from reactor (%)	81 ± 5
	Residual activity in reactors after extraction (%)	17 ± 4
	Duration (min)	15
Exchange solvent to MeCN and concentrate to <0.1 mL	Activity before loading on cartridge (%)	81 ± 5
	Activity trapped on light C18 (%)	52 ± 10
	Waste from trapping and washing process (%)	27 ± 11
	Eluted activity with 0.5 mL of MeCN (%)	51 ± 10
	Residue activity on cartridge (%)	1 ± 0
	Duration of the solvent-exchange process (min)	10
	Duration of MeCN evaporation	5
Purification	Isolated [^{18}F]YH149 from radio-HPLC (%)	50 ± 10
	Duration (min)	13
	Total preparation time (min)	58

3 Calibration curve to determine molar activity

The same analytical scale radio-HPLC system was used to determine the molar activity of the purified [^{18}F]YH149. The area under the curve for the UV absorbance peak was determined for a range of mole amounts of YH149 reference standard (0.06-0.98 nmol) to generate a linear calibration curve (**Figure S11**). This curve was then used to determine the mass of YH149 in the unknown sample, and subsequently compute the molar activity, following standard procedures.

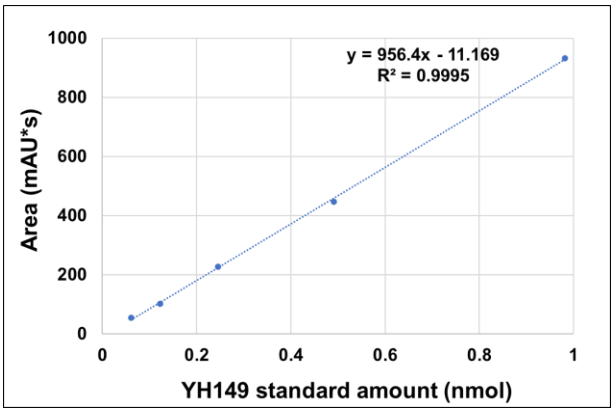

Figure S11. Calibration curve of YH149 reference standard (254 nm wavelength).

4 Example HPLC chromatograms from translated synthesis

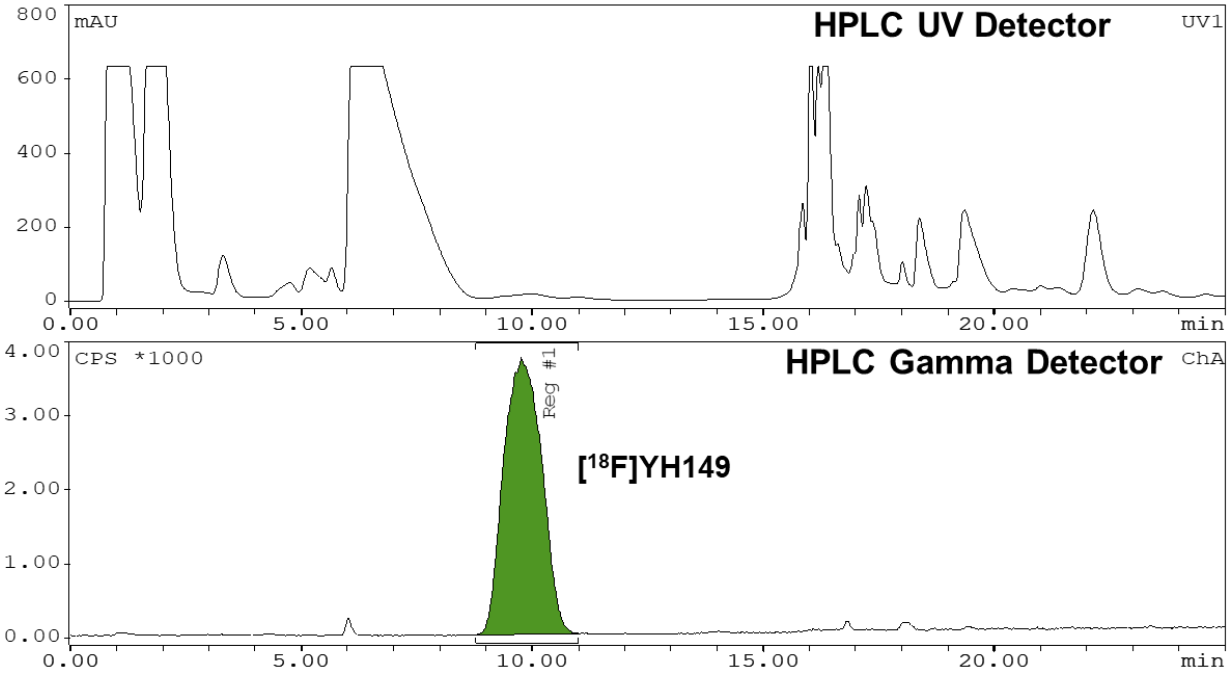

Figure S12. Example radio-HPLC chromatogram of crude [^{18}F]YH149 from macroscale radiosynthesis. The retention time was 10.0 min, earlier than that with microscale purification (t_R=18.6 min) because the crude sample was injected in 100 µL MeCN (versus 80 µL of the HPLC mobile phase for the microscale synthesis).

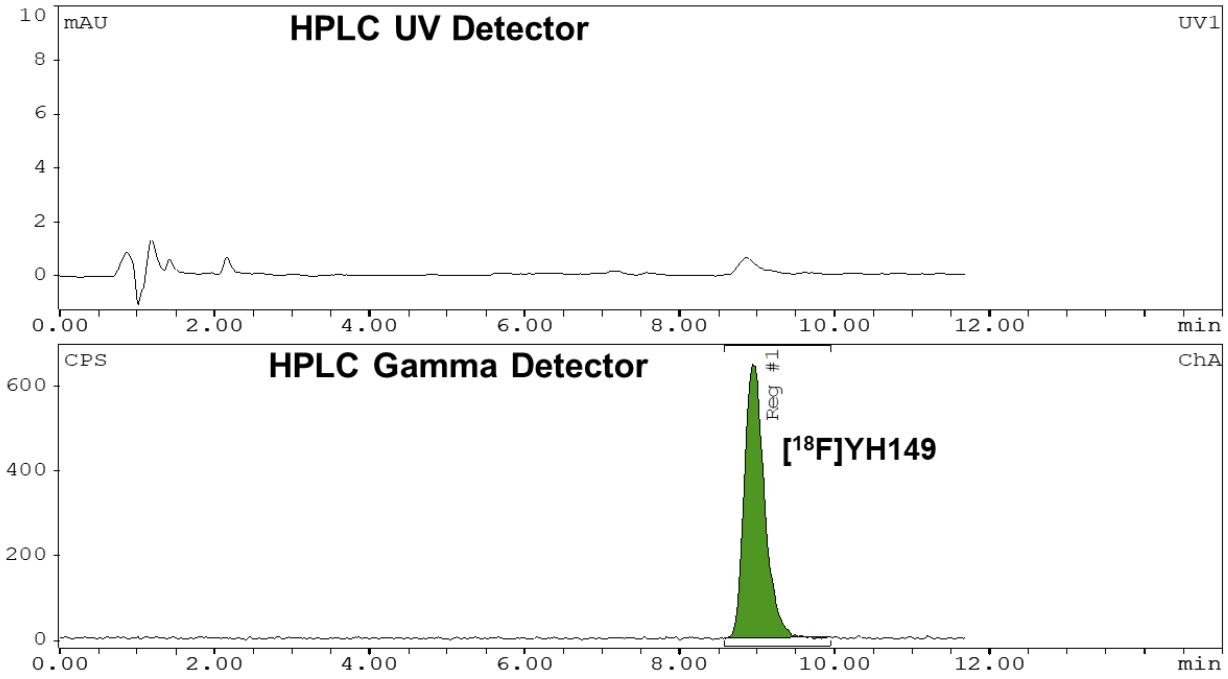

Figure S13. Example radio-HPLC chromatogram of purified [^{18}F]YH149 from macroscale radiosynthesis.

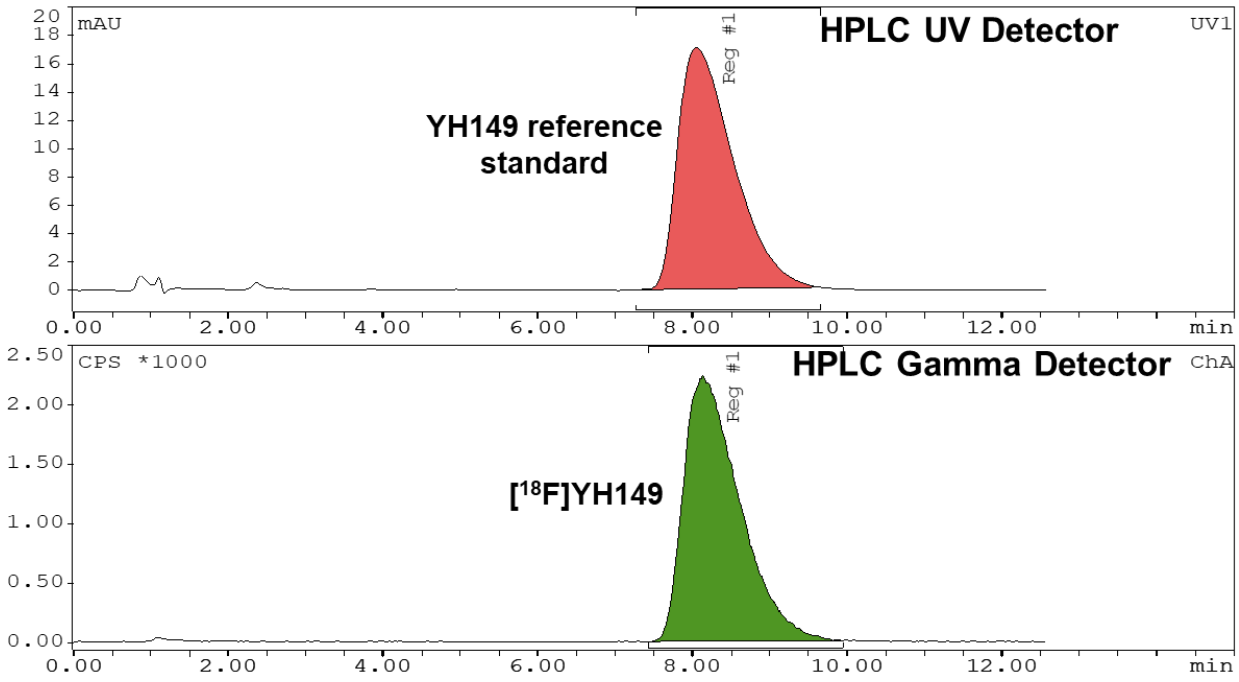

Figure S14. Example radio-HPLC chromatogram of co-injection of purified [^{18}F]YH149 (from macroscale radiosynthesis) and reference standard.

5 References

1 Y. He, M. Schild, U. Grether, J. Benz, L. Leibrock, D. Heer, A. Topp, L. Collin, B. Kuhn, M. Wittwer, C. Keller, L. C. Gobbi, R. Schibli and L. Mu, *J. Med. Chem.*, 2022, **65**, 2191–2207.

2 Y. Lu and R. M. van Dam, *Nuclear Medicine and Biology*, 2021, **96–97**, S15–S16.